N^6-methyladenosine (m^6A) and reader protein YTHDF2 enhance innate immune response by mediating DUSP1 mRNA degradation and activating mitogen-activated protein kinases during bacterial and viral infections

Jian Feng,[a,b] Wen Meng,[a,b] Luping Chen,[a,b] Xinquan Zhang,[a,b] Ashley Markazi,[a,b] Weiming Yuan,[c] Yufei Huang,[a,d,e,f] Shou-Jiang Gao[a,b]

[a]Cancer Virology Program, UPMC Hillman Cancer Center, University of Pittsburgh, Pittsburgh, PA, USA

[b]Department of Microbiology and Molecular Genetics, University of Pittsburgh, Pittsburgh, PA, USA

[c]Department of Molecular Microbiology and Immunology, Keck School of Medicine, University of Southern California School of Medicine, Los Angeles, CA, USA

[d]Department of Electrical and Computer Engineering, University of Pittsburgh, Pittsburgh, PA, USA

[e]Department of Biomedical Informatics, University of Pittsburgh, Pittsburgh, PA, USA

[f]Department of Medicine, University of Pittsburgh, Pittsburgh, PA, USA

Address correspondence to Shou-Jiang Gao, gaos8@upmc.edu.

The authors declare no conflict of interest.

Abstract

Mitogen-activated protein kinases (MAPKs) play critical roles in the induction of numerous cytokines, chemokines, and inflammatory mediators that mobilize the immune system to counter pathogenic infections. Dual-specificity phosphatase-1 (DUSP1) is a member of dual-specificity phosphatases, which inactivates MAPKs through a negative feedback mechanism. Here we report that in response to viral and bacterial infections, not only DUSP1 transcript but also its N^6-methyladenosine (m^6A) level rapidly increase together with the m^6A reader protein YTHDF2, resulting in enhanced YTHDF2-mediated DUSP1 transcript degradation. Knockdown of DUSP1 promotes p38 and JNK phosphorylation and activation, thus increasing the expression of innate immune response genes including IL1β, CSF3, TGM2 and SRC. Similarly, knockdown of m^6A eraser ALKBH5 increases DUSP1 transcript m^6A level resulting in accelerated transcript degradation, activation of p38 and JNK, and enhanced expression of IL1β, CSF3, TGM2 and SRC. These results demonstrate that m^6A and reader protein YTHDF2 orchestrate optimal innate immune response during viral and bacterial infections by downregulating the expression of a negative regulator DUSP1 of the p38 and JNK pathways that are central to innate immune response against pathogenic infections.

IMPORTANCE

Innate immunity is central for controlling pathogenic infections and maintaining the homeostasis of the host. In this study, we have revealed a novel mechanism regulating innate immune response during viral and bacterial infections. We have found that N^6-methyladenosine (m^6A) and the reader protein YTHDF2 regulate dual-specificity phosphatase-1, a negative regulator of mitogen-activated protein kinases p38 and JNK, to maximize innate immune response during viral and bacterial infections. These results provide novel insights into the mechanism regulating innate immunity, which could help the development of novel approaches for controlling pathogenic infections.

KEYWORDS: N^6-methyladenosine, m^6A; YTHDF2; Innate immunity; dual-specificity phosphatase-1, DUSP1; mitogen-activated protein kinases, MAPKs; p38; JNK

Introduction

The innate immune system is a highly efficient cellular and molecular network in mammalian cells that protects the organism against pathogenic infections (1). This first line of defense against invasion is achieved by sensing the pathogens through pattern recognition receptors (2). Stimulation of pattern recognition receptors on the cell surface and in the cytoplasm of innate immune cells activates multiple mitogen-activated protein kinases (MAPKs) including the extracellular signal-regulated kinase (ERK), p38 and Jun N-terminal kinase (JNK) (3). MAPKs are a group of highly conserved serine/threonine protein kinases in eukaryotes (4), which play a critical role in inducing numerous cytokines, chemokines, and inflammatory mediators that mobilize the immune system to counter pathogenic infections (5). Furthermore, the induction of pro-inflammatory response promotes the recruitment of additional immune cells to invoke secondary innate and adaptive immune responses (6).

Dual-specificity phosphatase-1 (DUSP1, also known as MAPK phosphatase-1 or MKP-1) was initially identified in cultured murine cells (7). It is a member of dual-specificity phosphatases (DUSPs), which are key players for inactivating different MAPKs (8). DUSP1 expression is enhanced upon numerous pathogenic infections, and it is an important feedback mechanism for controlling excessive immune response and inflammation (9, 10). By dephosphorylation, DUSP1 inhibits the activation of specific threonine and

tyrosine residues on p38 and JNK, resulting in inactivation of inflammatory or innate immune response through inhibiting the expression of numerous effector genes at transcriptional or post-transcriptional levels (11).

N6-methyladenosine (m^6A), a dynamic posttranscriptional RNA modification, is critical for almost all aspects of RNA metabolism and functions including structure, maturation, stability, splicing, export, translation, and decay (12). Recent studies show that m^6A modification not only directly regulates the expression of innate immune response genes, but also indirectly affects the mRNA metabolism pathway to further regulate the innate immune response during bacterial and viral infections (13-16) .

We have previously shown that m^6A plays an important role in regulating innate immune response against both bacterial and viral infections by directly and indirectly regulating the expression of innate immune response genes (13). More recent works indicate m^6A is a vital factor for regulating innate immune response and cytokines by affecting the IKKε/TBK1/IRF3, MAPK and NF-κB pathways (17, 18). In this study, we have discovered that DUSP1 is a direct m^6A target, and m^6A and the reader protein YTHDF2 regulate DUSP1 stability to maximize innate immune response during bacterial and viral infections.

Results

m^6A mediates DUSP1 transcript expression during bacterial

infection. We have previously mapped the cellular expression profiles and m^6A epitranscriptomes, and identified a set of genes including innate immune response genes that are differentially methylated and differentially expressed during viral and bacterial infections (13). Among them, DUSP1, an important regulator of innate immune response genes, was significantly hyper-methylated during gram-negative bacteria *Pseudomonas aeruginosa* infection, which peaked at 2 h post-infection (hpi), then decreased at 4 and 6 hpi (Fig. 1A). At the same time, DUSP1 transcript expression was upregulated which also peaked at 2 hpi, then decreased at 4 and 6 hpi (Fig. 1B). These results were consistent with the induction of DUSP1 by LPS or TLR ligands reported in previous studies (19, 20).

We confirmed the increase of DUSP1 transcript m^6A during *P. aeruginosa* infection by m^6A-immunoprecipitation reverse transcription quantitative real time PCR (MeRIP-qPCR). The DUSP1 transcript m^6A level was increased by 2.3-fold at 2 hpi of *P. aeruginosa* but then decreased at 4 and 6 hpi (Fig. 1C). Reverse transcription quantitative real time PCR (RT-qPCR) further confirmed the increased DUSP1 transcript expression following *P. aeruginosa* infection, which peaked at 2 hpi (Fig. 1D).

We then performed knockdown of ALKBH5, an m^6A “eraser”, to determine whether the increase of DUSP1 transcript m^6A could affect its expression (Fig. 1E). As expected, ALKBH5 knockdown further increased the m^6A level of DUSP1 transcript by 2.5- to 2.8-fold (Fig. 1F). However, DUSP1

123 transcript expression was reduced by 25% to 40% (Fig. 1G), which was also
124 reflected in the decreased DUSP1 protein level (Fig. 1E). These results
125 suggest that the increased m^{6}A level during *P. aeruginosa* infection likely
126 serves to reverse the upregulation of DUSP1 transcript. Since one of the
127 functions of m^{6}A modification is to mediate RNA decay (21, 22), we examined
128 DUSP1 transcript stability during *P. aeruginosa* infection. The half-life of
129 DUSP1 transcript was reduced by 12.7% to 37.1% following ALKBH5
130 knockdown (Fig. 1H), indicating m^{6}A regulation of DUSP1 RNA decay during *P.*
131 *aeruginosa* infection.
132
133 **YTHDF2 mediates m^{6}A-dependent DUSP1 transcript degradation.**
134 In order to further delineate the role of m^{6}A in innate immune response, we
135 infected mouse RAW264.7 macrophage cells with different doses of
136 gram-negative or -positive bacteria or human simplex virus type 1 (HSV-1),
137 and examined the expression of innate immune response genes (Fig. S1).
138 Infection with 10^7 gram-positive bacteria *Corynebacterium diphtheriae*, 10^7 *P.*
139 *aeruginosa* or 1 multiplicity of infection (MOI) of HSV-1 induced maximum
140 expression of innate immune response genes including colony stimulating
141 factor 3 (CSF3), interleukin-1β (IL1β), transglutaminase 2 (TGM2),
142 proto-oncogene tyrosine-protein kinase Src (SRC) under our experimental
143 conditions (Fig. S1). Thus, we used these conditions in subsequent
144 experiments.

We examined the protein levels of m^{6}A "writers", "erasers" and "readers" during bacterial and viral infections (Fig. 2A). The m^{6}A "writer" protein METTL14 had marginal increases during *P. aeruginosa, C. diphtheriae* and wild-type (WT) HSV-1 infections while another m^{6}A "writer" protein METTL3 had marginal increases during *P. aeruginosa* and *C. diphtheriae* infections (Fig. 2A). The eraser protein ALKBH5 also had slight increase during *C. diphtheriae* infection. Of the reader proteins examined, YTHDF1 had marginal increase during *C. diphtheriae* infection. However, YTHDF2 had significant increases during *C. diphtheriae* and *P. aeruginosa* infections by 3.89- and 4.21-fold, respectively, at 8 hpi (Fig. 2A). Since YTHDF2 mediates m^{6}A-dependent RNA decay (23), we performed knockdown of YTHDF2 (Fig. 2B), and observed an upregulation of the DUSP1 transcript (Fig. 2C), which was also reflected in an increase of DUSP1 protein level (Fig. 2B). Knockdown of YTHDF2 almost doubled the half-life of DUSP1 transcript (Fig. 2D). Furthermore, YTHDF2 RNA immunoprecipitation reverse transcription quantitative real time PCR (RIP-qPCR) showed the binding of YTHDF2 protein to the DUSP1 RNA transcript, which was significantly increased at 4 and 6 hpi (Fig. 2E), correlating with the increased YTHDF2 protein level at these time points (Fig. 2A). Together, these results indicate that the upregulation of YTHDF2 protein promotes the degradation of DUSP1 transcript during *P. aeruginosa* infection.

DUSP1 regulates p38 and JNK phosphorylation during bacterial

and viral infections. As an important innate immune response gene, DUSP1 inactivates MAPKs by inhibiting their phosphorylation (11). Our results showed upregulation of DUSP1 transcript during bacterial and viral infections, which was reversed by m^6A- and YTHDF2-mediated transcript degradation (Fig. 1 and 2). As expected, ERK, p38 and JNK MAPKs were activated at 2 hpi by *P. aeruginosa*, *C. diphtheriae*, and HSV-1 WT and ICP34.5 mutant viruses (Fig. 3A). We included the HSV-1 ICP34.5 mutant virus because the ICP34.5 protein has been shown to prevent the induction of innate immune genes during HSV-1 infection by directly inhibiting TBK1 activation and eIF2a function (24, 25). To determine whether DUSP1 regulated the activation of MAPKs during bacterial and viral infections, we performed DUSP1 knockdown. Western-blotting results showed that the levels of phosphorylated p38 and JNK (p-p38 and p-JNK) were increased following DUSP1 knockdown during bacterial and viral infections (Fig. 3A). Activation of MAPKs can induce their downstream transcriptional factors including AP-1 and C/EBP, resulting in upregulation of target genes including numerous innate immune response genes (26). Consistent with the increased levels of p-p38 and p-JNK following DUSP1 knockdown, the levels of CSF3, IL1β, TGM2 and SRC transcripts were upregulated (Fig. 3B). We observed some variations of the effects of different DUSP1 siRNAs on the expression of IL1β, CSF3, TGM2 and SRC transcripts. These might be due to the different knockdown kinetics of these siRNAs. The IL1β protein level was also upregulated after DUSP1 knockdown during

infections by *P. aeruginosa*, *C. diphtheriae*, and HSV-1 ICP34.5 mutant virus (Fig. 3C). However, upregulation of the IL1β protein was weak during WT HSV-1 infection and its increase was only marginal after DUSP1 knockdown (Fig. S2A), which was likely due to the inhibition of innate immune response by the HSV-1 ICP34.5 protein (24, 25). These results indicated that DUSP1 inhibited p-p38 and p-JNK activation to block innate immune response during bacterial and viral infections.

ALKBH5 regulates p38 and JNK phosphorylation, and their downstream innate immune response genes during bacterial and viral infections. Since DUSP1 inactivated the p38 and JNK during bacterial and viral infections, and ALKBH5 knockdown reduced DUSP1 transcript stability by increasing m^6A level, we examined ALKBH5 regulation of p38 and JNK activation. ALKBH5 knockdown increased the levels of p-p38 and p-JNK during infection by *P. aeruginosa*, *C. diphtheriae*, or HSV-1 WT or ICP34.5 mutant virus (Fig. 4A-4D). Some minor increase of p-ERK was also observed at 2 hpi of *C. diphtheriae*. Since the increased p-p38 and p-JNK levels could lead to enhanced activation of their downstream transcriptional factors, we examined *de novo* transcription of the target genes by performing nuclear run-on assay during *P. aeruginosa* infection. ALKBH5 knockdown indeed increased the transcriptional activities of IL1β, CSF3, TGM2 and SRC genes (Fig. 4E).

We further examined the role of ALKBH5 on the expression of innate immune response genes. ALKBH5 knockdown increased the levels of IL1β, CSF3, TGM2 and SRC transcripts during infection by *P. aeruginosa*, *C. diphtheriae*, or HSV-1 WT or ICP34.5 mutant virus (Fig. 5A). Similar to DUSP1 knockdown, we noticed variations of the effects of different ALKBH5 siRNAs on both the transcription and expression of IL1β, CSF3, TGM2 and SRC genes (Fig. 4E and 5). These might be due to the different knockdown kinetics of these siRNAs, which might impact the m^6A level of DUSP1 transcript, DUSP1 expression level, and p-p38 and p-JNK levels, leading to variable transcription and expression levels of these downstream genes.

The protein level of IL1β was also upregulated after ALKBH5 knockdown during infections by *P. aeruginosa*, *C. diphtheriae*, and HSV-1 ICP34.5 mutant virus (Fig. 5B-5D). However, the upregulation of IL1β protein was marginal during WT HSV-1 infection (Fig. S2B). In contrast, overexpression of ALKBH5 reduced the levels of IL1β, CSF3, TGM2 and SRC transcripts (Fig. 5E), and downregulated the IL1β protein level (Fig. 5F) during *P. aeruginosa* infection. It was interesting that the reduced expression of the four transcripts had different kinetics following overexpression of ALKBH5 (Fig. 5E). The effect of ALKBH5 overexpression was observed for TGM2 and SRC transcripts at as early as 2 hpi, which disappeared by 6 hpi. However, the effect was not observed for CSF3 until 4 hpi and for IL1β until 6 hpi. It is possible that the promoters of these genes might endow them with different

kinetics in response to the activation of p38 and JNK pathways.

Because our results showed an important role of ALKBH5 in regulating innate immune response, we further examined the impact of ALKBH5 knockdown on HSV-1 replication. ALKBH5 knockdown reduced the replication of HSV-1 WT or ICP34.5 mutant virus (Fig. S3). These results are in agreement with those of a previous study showing reduced HSV-1 replication after ALKBH5 knockout (14).

In conclusion, bacterial and viral infections activate MAPKs to induce innate immune response genes as well as a negative regulator of MAPKs, DUSP1, to avoid excessive innate immune response. At the same time, numerous m^6A writer proteins and reader protein YTHDF2 are induced, leading to hyper-methylation of DUSP1 transcript, which is targeted for YTHDF2-mediated degradation. This mechanism of fine-tuned activation of MAPKs optimizes the induction of innate immune response genes during pathogenic infections (Fig. 6).

Discussion

The innate immune system is a complex cellular and molecular network in mammalian cells that serves as the first line of defense against pathogenic infections and is regulated by diverse cellular pathways (1). DUSP1 is a critical regulator of MAPK pathways serving as a negative feedback mechanism to prevent excessive activation of these pathways (27, 28). In the context of

pathogenic infections, activation of MAPKs induces the expression of innate immune response genes as well as DUSP1, which prevents overreactive immune response (29-31). Our results showed that DUSP1 transcript was indeed induced during bacterial and viral infections together with the activation of the ERK, JNK and p38 MAPK pathways. At the same time, the m^6A level of DUSP1 transcript was significantly increased. During these processes, we only observed marginal increases of m^6A writer proteins METTL3 and METTL14 and no decrease of m^6A eraser proteins ALKBH5 and FTO, suggesting that the observed m^6A increase in the DUSP1 transcript likely depended on preexisting writer proteins. Interestingly, despite the increased expression of DUSP1 transcript during bacterial and viral infections, we failed to detect an increase of DUSP1 protein. It is unclear whether the increased DUSP1 transcript m^6A might affect its translation. In addition, it is unclear why the m^6A level is only increased in some *de novo* transcribed transcripts but not others. The specific mechanism involved in this selection process might deserve further investigations. Nevertheless, the results of ALKBH5 knockdown experiments revealed that the m^6A increase in the DUSP1 transcript targeted it for YTHDF2-mediated degradation. Importantly, YTHDF2 was significantly induced during bacterial infections, which maximized its negative regulation of DUSP1 transcript stability. Taken together, these results suggest that m^6A and YTHDF2 are involved in fine-tuning the expression of DUSP1 protein, an important regulator of innate immunity, during pathogenic infections.

The observed induction of YTHDF2 protein is consistent with results from another study showing LPS induction of YTHDF2 expression (32). Interestingly, there was no obvious change of YTHDF2 protein following HSV-1 infection, indicating possible involvement of the bacteria-associated pattern recognition receptors in the induction of YTHDF2 protein. However, it is possible that HSV-1 infection might have a YTHDF2 induction kinetic that is different from those of bacterial infections. Alternatively, HSV-1 might have evolved to prevent YTHDF2 induction as a mechanism to counter innate immune response.

Our results showed that m^6A- and YTHDF2-mediated degradation of DUSP1 transcript resulted in enhanced activation of p38 and JNK. Both p38 and JNK pathways activate transcriptional factors such AP-1 and C/EBP that are essential for the expression of innate immune response genes. Indeed, knockdown DUSP1 or m^6A eraser ALKBH5 enhanced the expression of innate immune response genes including IL1β, CSF3, TGM2 and SRC during bacterial or viral infections. We observed robust induction of the IL1β precursor by HSV-1 ICP34.5 mutant but not WT virus (Fig. S2). It has been reported that the ICP34.5 protein can directly inhibit TBK1 and eIF2a proteins to prevent the induction of innate immune genes during HSV-1 infection (24, 25). Interestingly, activated MAPK pathways can promote HSV-1 viral replication by activating downstream transcriptional factors (33, 34). However, we showed that ALKBH5 knockdown inhibited HSV-1 replication, which was likely due to

299 m^{6}A-mediated downregulation of DUSP1 and subsequent activation of MAPK
300 pathways resulting in the induction of innate immune response. However, it is
301 also possible that ALKBH5 and m^{6}A might regulate HSV-1 replication through
302 another mechanism in addition to targeting DUSP1 transcript for degradation
303 and activating MAPK pathways.

304 We have previously shown that a set of innate immune response genes
305 are subjected to m^{6}A modification and might be directly regulated by m^{6}A while
306 another set of innate immune response genes might be indirectly regulated by
307 m^{6}A during bacterial and viral infections (13). In the current work, we have
308 provided an example of m^{6}A and YTHDF2 indirect regulation of innate immune
309 response genes by mediating the stability of DUSP1 transcript. In fact, DUSP1
310 is under the tight control of m^{6}A and YTHDF2 during bacterial and viral
311 infections. It can be speculated that other DUSP genes, which are involved in
312 diverse cellular functions, could also be regulated by m^{6}A and m^{6}A-related
313 proteins, and therefore deserve further investigations.

314

315 **Material and methods**

316 **Bacteria, viruses, and cells.** *P. aeruginosa* and *C. diphtheriae* were
317 purchased from ATCC. Herpes simplex virus type 1 (HSV-1) F strain and
318 HSV-1 ICP34.5 mutant virus were obtained from Dr. Bernard Roizman (The
319 University of Chicago, Chicago, IL). The ICP34.5 mutant virus (R3616) was
320 generated by deleting the 1 kb fragment containing both copies of the gamma

34.5 gene between the BstEII and Stu I sites from the F strain HSV-1 genome (35). RAW 264.7 cells were purchased from ATCC and cultured following the instructions of the vendor.

Bacteria and virus infection. RAW 264.7 cells at 4×10^5 cells per mL were infected with *P. aeruginosa* or *C. diphtheriae* at 10^7 per mL, or with HSV-1 WT or ICP34.5 mutant virus at 1 MOI. Cells were harvested at the indicated time points.

m^{6}A-immunoprecipitation (m^{6}A-IP). Isolation of m^{6}A-containing fragments was performed as previously described (13, 36). Briefly, total RNA was extracted from cells using TRI Reagent (T9424-200ML, Sigma-Aldrich) and fragmented using RNA fragmentation kit (AM8740, ThermoFisher). Successful fragmentation of RNA with sizes close to 100 nucleotides was validated using bioanalyzer (2100 Bioanalyzer Instrument, Agilent). Anti-m^{6}A antibody (10 µg) (202-003, Synaptic Systems) was incubated with 30 µl slurry of Pierce Protein A Agarose beads (20365, ThermoFisher) by rotating in 250 µl PBS at 4 °C for 3 h. The beads were washed three times in cold PBS followed by one wash in IP buffer containing 10 mM Tris-HCl at pH 7.4, 150 mM NaCl, and 1% Igepal CA-630 (I8896-50ML, Sigma-Aldrich). To isolate the m^{6}A-containing fragments, 120 µg of fragmented total RNA was added to the antibody-bound beads in 250 µl IP buffer supplemented with RNasin Plus

RNase inhibitor (PRN2615, Promega), and the mixture was incubated at 4 °C for 2 h. The beads were washed seven times with 1 ml IP buffer and eluted with 100 µl IP buffer supplemented with 6.67 mM of m^6A salt (M2780, Sigma-Aldrich) at 4 °C for 1 h. A second elution was carried out and the eluates were pooled together before purification by ethanol 70% precipitation.

siRNA knockdown. siRNA silencing was performed by transfecting 2.5 pmol of each siRNA per well in a 12-well plate into the RAW264.7 cells using Lipofectamine RNAi Max (13778150, ThermoFisher) according to manufacturer's instructions. Two days after transfection, the cells were monitored for knockdown efficiency of the target gene by RT-qPCR and Western-blotting. siRNAs purchased from Sigma-Aldrich are as follows: DUSP1 si1: SASI_Mm02_00322441; DUSP1 si2: SASI_Mm01_00056586; DUSP1 si3: SASI_Mm01_00056587; ALKBH5 si1: SASI_Mm01_00106232; ALKBH5 si2: SASI_Mm02_00344968; ALKBH5 si3: SASI_Mm01_00106233; and siNegative Control (NC): Sigma siRNA Universal Negative Control #1 (SIC001-10NMOL).

RNA stability assay. Actinomycin D (10 µg/ml) (A9415-2MG, Sigma-Aldrich) was added to cells to inhibit transcription. RNA was isolated at 0, 2, 4 and 6 h after actinomycin D treatment using Trizol and the transcripts were quantified by RT-qPCR.

RT-qPCR for gene expression, RIP-qPCR for YTHDF2 RNA binding quantification and MeRIP-qPCR for m^{6}A-seq validation. Total RNA was isolated with TRI Reagent (T9424-200ML, Sigma-Aldrich) according to the manufacturer's instructions. Reverse transcription was performed with 1 μg of total RNA using Maxima H Minus First Strand cDNA Synthesis Kit (Cat.# K1652, ThermoFisher). Quantitative PCR was done using SsoAdvanced Universal SYBR Green Supermix (1725271, Bio-Rad). Relative gene expression levels were obtained by normalizing the cycle threshold (CT) values to yield $2^{-\Delta\Delta Ct}$ values. For validation of m^{6}A-seq, eluted or input mRNA was subjected to RT-qPCR. Fold enrichment was obtained by calculating the $2^{-\Delta Ct}$ value of eluate in relative to the input sample. The primers used for gene expression are:

5'CTGGTGGGTGTGTCAAGCAT3' (forward) and

5'GAGGCAGTTTCTTCGCTTGC3' (reverse) for DUSP1; and

5'CCCTGAAGTACCCCATTGAA3' (forward) and

5'GGGGTGTTGAAGGTCTCAAA3' (reverse) for β-actin; and

5'GAGTGTGGATCCCAAGCAAT3' (forward) and

5'ACGGATTCCATGGTGAAGTC3' (reverse) for IL1β; and

5'CCGGTACCCTCTCCTGTTGTGTTTA3' (forward) and

5'AACTCGAGCTAAAAAGGAGGACGGC3' (reverse) for CSF3; and

5'AAGAGCTCCAAACAAGGTCTGCCTT3' (forward) and

5'AACTCGAGACGTGCCATATAAGCAC3' (reverse) for TGM2; and

5'AAGGTACCCTGCCAGGCCAGACCAA3' (forward) and

5'AACTCGAGCCAGCCTTGACCCTGAG3' (reverse) for SRC; and

5'ACGGTTTACTACGCCGTGTT3' (forward) and

5'TGTAGGGTTGTTTCCGGACG3' (reverse) for US6; and

5'GACGAACATGAAGGGCTGGA' (forward) and

5'CGACCTGTTTGACTGCCTCT3' (reverse) for VP16; and

5'CCCACTATCAGGTACACCAGCTT3' (forward) and

5'CTGCGCTGCGACACCTT3' (reverse) for ICP0; and

5'GCATCCTTCGTGTTTGTCATTCTG3' (forward) and

5'GCATCTTCTCTCCGACCCCG3' (reverse) for ICP27.

Western-blotting. Protein samples were lysed in Laemmli buffer, separated by SDS-PAGE and transferred to a nitrocellulose membrane (37). The membrane was blocked with 5% milk and then incubated with primary antibody to GAPDH (5174s, CST), p38 (8690S, CST), p-p38 (4511S, CST), ERK (4695S, CST), p-ERK (4370S, CST), JNK (9252S, CST), p-JNK (4668S, CST), DUSP1 (NBP2-67909, Novus), IL1β (AB-401-NA, R&D system), or ALKBH5 (HPA007196, Sigma) overnight at 4 °C. The membrane was washed with TBS-Tween (TBS-T) and probed with a secondary antibody conjugated to horseradish peroxidase (HRP). After further washing with TBS-T, the blot was visualized using SuperSignal™ West Femto Maximum Sensitivity Substrate

(34096, Thermo) and imaged on a ChemiDoc™ MP Imaging System (12003154, Bio-Rad).

Nuclear run-on assay. Nuclear run-on assay was conducted as previously described (38).

RNA immunoprecipitation (RIP) assay. RIP assay was conducted as previously described (39).

SUPPLEMENTAL MATERIAL

Supplemental material is available online only.

FIG S1, PDF file, 0.5 MB.

FIG S2, PDF file, 1 MB.

FIG S3, PDF file, 0.8 MB.

ACKNOWLEDGMENTS

This work was supported by grants from the National Institutes of Health (CA096512 and CA124332 to S.-J. Gao), and in part by award P30CA047904.

We thank members of Dr. Shou-Jiang Gao's laboratory for technical assistance and helpful discussions.

J.F. performed most of the experiments. W.M., L.P.C., X.Q.Z. and A.M. performed a subset of experiments. Y.F.H. performed the bioinformatic

analysis. W.Y. provides the HSV-1 wild-type and mutant viruses. J.F. and S.J.G. prepared the manuscript. S.J.G. planned, managed, and supervised the study, and secured funding.

REFERENCES

1. Akira S, Uematsu S, Takeuchi O. 2006. Pathogen recognition and innate immunity. Cell 124:783-801.
2. Medzhitov R, Janeway C, Jr. 2000. Innate immunity. N Engl J Med 343:338-44.
3. Arthur JS, Ley SC. 2013. Mitogen-activated protein kinases in innate immunity. Nat Rev Immunol 13:679-92.
4. Nishida E, Gotoh Y. 1993. The MAP kinase cascade is essential for diverse signal transduction pathways. Trends Biochem Sci 18:128-31.
5. Dong C, Davis RJ, Flavell RA. 2002. MAP kinases in the immune response. Annu Rev Immunol 20:55-72.
6. Iwasaki A, Medzhitov R. 2010. Regulation of adaptive immunity by the innate immune system. Science 327:291-5.
7. Charles CH, Abler AS, Lau LF. 1992. cDNA sequence of a growth factor-inducible immediate early gene and characterization of its encoded protein. Oncogene 7:187-90.
8. Theodosiou A, Ashworth A. 2002. MAP kinase phosphatases. Genome Biol 3:REVIEWS3009.
9. Bode JG, Ehlting C, Haussinger D. 2012. The macrophage response towards LPS and its control through the p38(MAPK)-STAT3 axis. Cell Signal 24:1185-94.
10. Caceres A, Perdiguero B, Gomez CE, Cepeda MV, Caelles C, Sorzano CO, Esteban M. 2013. Involvement of the cellular phosphatase DUSP1 in vaccinia virus infection. PLoS Pathog 9:e1003719.
11. Abraham SM, Clark AR. 2006. Dual-specificity phosphatase 1: a critical regulator of innate immune responses. Biochem Soc Trans 34:1018-23.
12. Tan B, Gao SJ. 2018. The RNA Epitranscriptome of DNA Viruses. J Virol 92:e00696-18.
13. Feng J, Zhang T, Sorel O, Meng W, Zhang X, Lai Z, Yuan W, Chen Y, Huang Y, Gao SJ. 2022. Global profiling reveals common and distinct N6-methyladenosine (m6A) regulation of innate immune responses during

bacterial and viral infections. Cell Death Dis 13:234.

14. Liu Y, You Y, Lu Z, Yang J, Li P, Liu L, Xu H, Niu Y, Cao X. 2019. N (6)-methyladenosine RNA modification-mediated cellular metabolism rewiring inhibits viral replication. Science 365:1171-1176.
15. Wang L, Wen M, Cao X. 2019. Nuclear hnRNPA2B1 initiates and amplifies the innate immune response to DNA viruses. Science 365:eaav0758.
16. Zheng Q, Hou J, Zhou Y, Li Z, Cao X. 2017. The RNA helicase DDX46 inhibits innate immunity by entrapping m(6)A-demethylated antiviral transcripts in the nucleus. Nat Immunol 18:1094-1103.
17. Jin S, Li M, Chang H, Wang R, Zhang Z, Zhang J, He Y, Ma H. 2022. The m6A demethylase ALKBH5 promotes tumor progression by inhibiting RIG-I expression and interferon alpha production through the IKKepsilon/TBK1/IRF3 pathway in head and neck squamous cell carcinoma. Mol Cancer 21:97.
18. Zheng Y, Li Y, Ran X, Wang D, Zheng X, Zhang M, Yu B, Sun Y, Wu J. 2022. Mettl14 mediates the inflammatory response of macrophages in atherosclerosis through the NF-kappaB/IL-6 signaling pathway. Cell Mol Life Sci 79:311.
19. Clark AR, Martins JR, Tchen CR. 2008. Role of dual specificity phosphatases in biological responses to glucocorticoids. J Biol Chem 283:25765-9.
20. Ichikawa T, Zhang J, Chen K, Liu Y, Schopfer FJ, Baker PR, Freeman BA, Chen YE, Cui T. 2008. Nitroalkenes suppress lipopolysaccharide-induced signal transducer and activator of transcription signaling in macrophages: a critical role of mitogen-activated protein kinase phosphatase 1. Endocrinology 149:4086-94.
21. Du H, Zhao Y, He J, Zhang Y, Xi H, Liu M, Ma J, Wu L. 2016. YTHDF2 destabilizes m(6)A-containing RNA through direct recruitment of the CCR4-NOT deadenylase complex. Nat Commun 7:12626.
22. Hsu PJ, Zhu Y, Ma H, Guo Y, Shi X, Liu Y, Qi M, Lu Z, Shi H, Wang J, Cheng Y, Luo G, Dai Q, Liu M, Guo X, Sha J, Shen B, He C. 2017. Ythdc2 is an N(6)-methyladenosine binding protein that regulates mammalian spermatogenesis. Cell Res 27:1115-1127.
23. Wang X, Lu Z, Gomez A, Hon GC, Yue Y, Han D, Fu Y, Parisien M, Dai Q, Jia G, Ren B, Pan T, He C. 2014. N6-methyladenosine-dependent regulation of messenger RNA stability. Nature 505:117-20.
24. Liu X, Ma Y, Voss K, van Gent M, Chan YK, Gack MU, Gale M, Jr., He B. 2021. The herpesvirus accessory protein gamma134.5 facilitates viral replication by disabling mitochondrial translocation of RIG-I. PLoS Pathog 17:e1009446.

25. Manivanh R, Mehrbach J, Knipe DM, Leib DA. 2017. Role of Herpes Simplex Virus 1 gamma34.5 in the Regulation of IRF3 Signaling. J Virol 91:e01156-17.

26. Dainichi T, Matsumoto R, Mostafa A, Kabashima K. 2019. Immune Control by TRAF6-Mediated Pathways of Epithelial Cells in the EIME (Epithelial Immune Microenvironment). Front Immunol 10:1107.

27. Gunzl P, Bauer K, Hainzl E, Matt U, Dillinger B, Mahr B, Knapp S, Binder BR, Schabbauer G. 2010. Anti-inflammatory properties of the PI3K pathway are mediated by IL-10/DUSP regulation. J Leukoc Biol 88:1259-69.

28. Salojin K, Oravecz T. 2007. Regulation of innate immunity by MAPK dual-specificity phosphatases: knockout models reveal new tricks of old genes. J Leukoc Biol 81:860-9.

29. Cornell TT, Fleszar A, McHugh W, Blatt NB, Le Vine AM, Shanley TP. 2012. Mitogen-activated protein kinase phosphatase 2, MKP-2, regulates early inflammation in acute lung injury. Am J Physiol Lung Cell Mol Physiol 303:L251-8.

30. Valente AJ, Yoshida T, Gardner JD, Somanna N, Delafontaine P, Chandrasekar B. 2012. Interleukin-17A stimulates cardiac fibroblast proliferation and migration via negative regulation of the dual-specificity phosphatase MKP-1/DUSP-1. Cell Signal 24:560-568.

31. Vattakuzhi Y, Abraham SM, Freidin A, Clark AR, Horwood NJ. 2012. Dual-specificity phosphatase 1-null mice exhibit spontaneous osteolytic disease and enhanced inflammatory osteolysis in experimental arthritis. Arthritis Rheum 64:2201-10.

32. Yu R, Li Q, Feng Z, Cai L, Xu Q. 2019. m6A Reader YTHDF2 Regulates LPS-Induced Inflammatory Response. Int J Mol Sci 20:1323.

33. Perkins D, Pereira EF, Gober M, Yarowsky PJ, Aurelian L. 2002. The herpes simplex virus type 2 R1 protein kinase (ICP10 PK) blocks apoptosis in hippocampal neurons, involving activation of the MEK/MAPK survival pathway. J Virol 76:1435-49.

34. Smith CC, Nelson J, Aurelian L, Gober M, Goswami BB. 2000. Ras-GAP binding and phosphorylation by herpes simplex virus type 2 RR1 PK (ICP10) and activation of the Ras/MEK/MAPK mitogenic pathway are required for timely onset of virus growth. J Virol 74:10417-29.

35. Chou J, Roizman B. 1994. Herpes simplex virus 1 gamma(1)34.5 gene function, which blocks the host response to infection, maps in the homologous domain of the genes expressed during growth arrest and DNA damage. Proc Natl Acad Sci U S A 91:5247-51.

36. Tan B, Liu H, Zhang S, da Silva SR, Zhang L, Meng J, Cui X, Yuan H,

546 Sorel O, Zhang SW, Huang Y, Gao SJ. 2018. Viral and cellular
547 N(6)-methyladenosine and N(6),2'-O-dimethyladenosine
548 epitranscriptomes in the KSHV life cycle. Nat Microbiol 3:108-120.

549 37. Gao SJ, Kingsley L, Li M, Zheng W, Parravicini C, Ziegler J, Newton R,
550 Rinaldo CR, Saah A, Phair J, Detels R, Chang Y, Moore PS. 1996. KSHV
551 antibodies among Americans, Italians and Ugandans with and without
552 Kaposi's sarcoma. Nat Med 2:925-8.

553 38. Patrone G, Puppo F, Cusano R, Scaranari M, Ceccherini I, Puliti A,
554 Ravazzolo R. 2000. Nuclear run-on assay using biotin labeling, magnetic
555 bead capture and analysis by fluorescence-based RT-PCR. Biotechniques
556 29:1012-4, 1016-7.

557 39. Hao H, Hao S, Chen H, Chen Z, Zhang Y, Wang J, Wang H, Zhang B, Qiu
558 J, Deng F, Guan W. 2019. N6-methyladenosine modification and METTL3
559 modulate enterovirus 71 replication. Nucleic Acids Res 47:362-374.

560

561 **Figure legend**

562 **FIG 1** m^{6}A mediates DUSP1 transcript stability during bacterial infection. (A)
563 Tracks of m^{6}A peaks on DUSP1 transcript at 0, 2, 4, and 6 hpi of *P. aeruginosa*.
564 (B) Expression levels of DUSP1 transcript at 0, 2, 4, and 6 hpi of *P. aeruginosa*
565 quantified by RNA-seq. (C) m^{6}A levels on DUSP1 transcript at 0, 2, 4, and 6
566 hpi of *P. aeruginosa* examined by MeRIP-qPCR. (D) Expression levels of
567 DUSP1 transcript at 0, 2, 4, and 6 hpi of *P. aeruginosa* quantified by RT-qPCR.
568 (E) Examination of DUSP1 and ALKBH5 protein levels following ALKBH5
569 knockdown in RAW264.7 cells by Western-blotting. (F) m^{6}A levels on DUSP1
570 transcript following ALKBH5 knockdown in RAW264.7 cells examined by
571 MeRIP-qPCR. (G) Expression levels of DUSP1 transcript following ALKBH5
572 knockdown in RAW264.7 cells examined by RT-qPCR. (H) Alterations of
573 half-lives of DUSP1 transcript following ALKBH5 knockdown in RAW264.7
574 cells during *P. aeruginosa* infection examined by RT-qPCR at the indicated
575 time points following addition of 10 μg/ml actinomycin D.

576

577 **FIG2** YTHDF2 mediates m^{6}A-dependent DUSP1 transcript stability during
578 bacterial and viral infections. (A) Protein levels of m^{6}A writers METTL3,
579 METTL14 and WTAP, erasers ALKBH5 and FTO, and readers YTHDF1 and
580 YTHDF2 with or without infection by *C. diphtheriae*, *P. aeruginosa* or HSV-1 at
581 the indicated time points examined by Western-blotting. (B) Examination of
582 DUSP1 and YTHDF2 protein levels following YTHDF2 knockdown in

583 RAW264.7 cells by Western-blotting. (C) Expression levels of DUSP1
584 transcript following YTHDF2 knockdown in RAW264.7 cells examined by
585 RT-qPCR. (D) Alterations of half-lives of DUSP1 transcript following YTHDF2
586 knockdown in RAW264.7 cells during *P. aeruginosa* infection examined by
587 RT-qPCR at the indicated time points following addition of 10 μg/ml
588 actinomycin D. (E) Binding of YTHDF2 to DUSP1 transcript at the indicated
589 time points following *P. aeruginosa* infection examined by RIP-qPCR.
590
591 **FIG 3** DUSP1 regulates p38 and JNK phosphorylation and expression of
592 innate immune response genes during bacterial and viral infections. (A)
593 DUSP1 knockdown enhanced the p38 and JNK phosphorylation during
594 infection of *P. aeruginosa*, *C. diphtheriae*, or HSV-1 or HSV-1 ICP34.5 mutant
595 virus. (B) DUSP1 knockdown enhanced the expression of IL1β, CSF3, TGM2
596 and SRC genes during infection of *P. aeruginosa*, *C. diphtheriae*, or HSV-1 or
597 HSV-1 ICP34.5 mutant virus. (C) DUSP1 knockdown enhanced the protein
598 level of IL1β during infection of *P. aeruginosa*, *C. diphtheriae* or HSV-1 ICP34.5
599 mutant virus.
600
601 **FIG 4** ALKBH5 regulates p38 and JNK phosphorylation and transcription of
602 innate immune response genes during bacterial and viral infections. (A-D)
603 ALKBH5 knockdown enhanced the p38 and JNK phosphorylation during
604 infection of *C. diphtheriae* (A), *P. aeruginosa* (B), or HSV-1 (C) or HSV-1

ICP34.5 mutant virus (D). (E) *De novo* transcription of IL1β, CSF3, TGM2 and SRC genes following ALKBH5 knockdown at 2 hpi of *P. aeruginosa* examined by nuclear run-on assay. Cells treated with 4-thiouridine for 1 h after ALKBH5 knockdown were infected *P. aeruginosa* for 4 h and collected for nuclear run-on assay.

FIG 5 ALKBH5 regulates the expression of innate immune response genes during bacterial and viral infections. (A) ALKBH5 knockdown enhanced the expression levels of IL1β, CSF3, TGM2 and SRC transcripts during *P. aeruginosa*, *C. diphtheriae*, or HSV-1 or HSV-1 ICP34.5 mutant virus infection. (B-D) ALKBH5 knockdown enhanced the protein level of IL1β during infection by *C. diphtheriae* (B), *P. aeruginosa* (C), or HSV-1 ICP34.5 mutant virus (D). (E) ALKBH5 overexpression inhibited the expression of IL1β, CSF3, TGM2 and SRC genes during *P. aeruginosa* infection measured by RT-qPCR. (F) ALKBH5 overexpression inhibited the protein level of IL1β during *P. aeruginosa* infection measured by Western-blotting.

FIG 6 A working model of regulation of DUSP1, MAPKs and innate immune response genes by m^6A and m^6A-related proteins YTHDF2 and ALKBH5 during pathogenic infections.

626 **SUPPLEMENTAL MATERIAL**

627 **FIG S1** Expression of CSF3, IL1β, TGM2 and SRC transcripts following
628 infection with different doses of *C. diphtheriae*, *P. aeruginosa* or HSV-1 at the
629 indicated time points examined by RT-qPCR.

630

631 **FIG S2** Protein level of IL1β precursor following knockdown of DUSP1 (A) or
632 ALKBH5 (B) at different time points following HSV-1 infection.

633

634 **FIG S3** ALKBH5 knockdown inhibits HSV-1 replication. RAW264.7 cells
635 transfected with ALKBH5 shRNAs or a scrambled control (NC) were infected
636 with 1 MOI of HSV-1 for 48 h, and the supernatants were collected for plaque
637 assay to determine the viral titers.

Figure 1

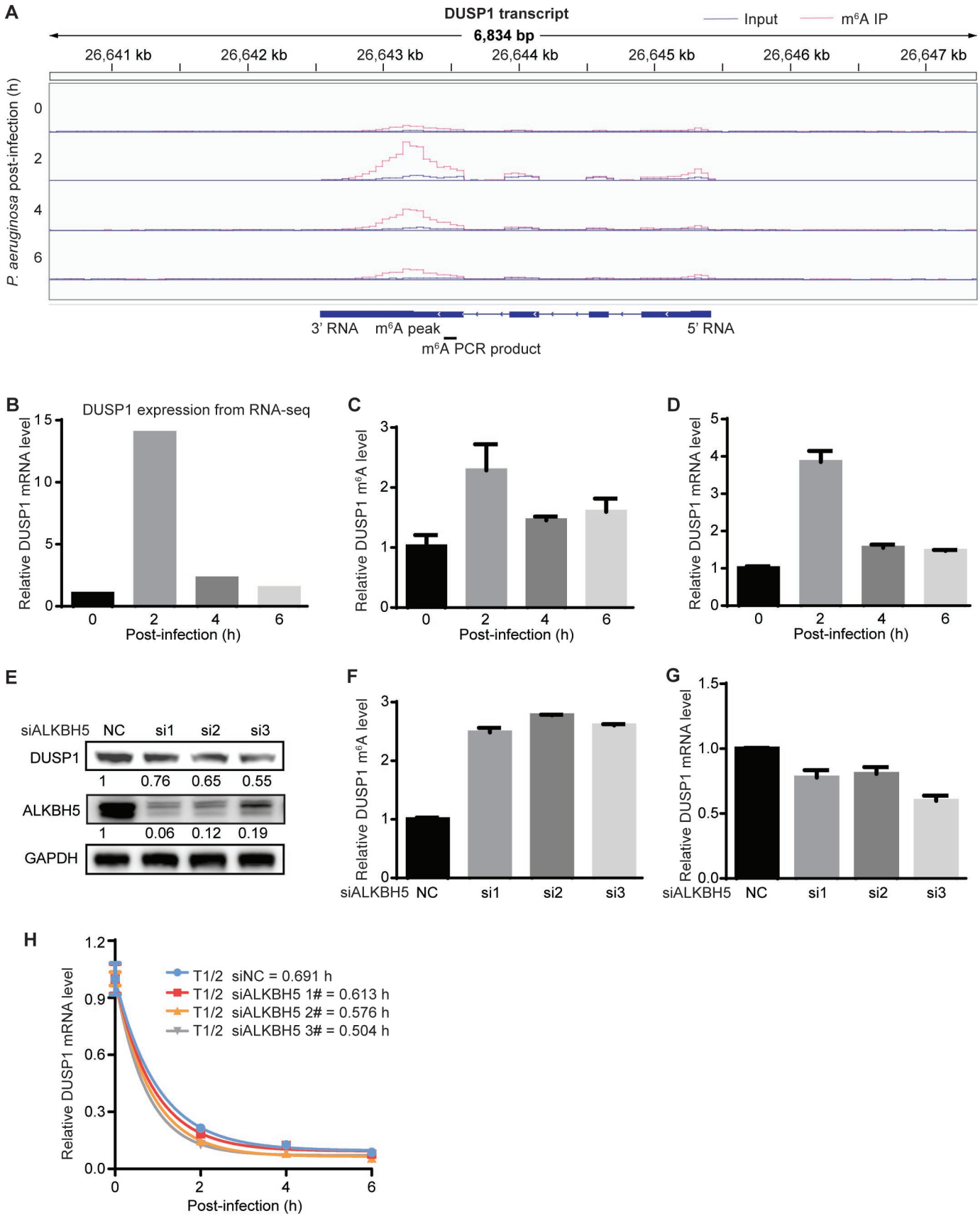
A
DUSP1 transcript
6,834 bp
Input
m6A IP
26,641 kb
26,642 kb
26,643 kb
26,644 kb
26,645 kb
26,646 kb
26,647 kb
P. aeruginosa post-infection (h)
0
2
4
6
3' RNA
m6A peak
5' RNA
m6A PCR product
B
DUSP1 expression from RNA-seq
Relative DUSP1 mRNA level
Post-infection (h)
C
Relative DUSP1 m6A level
Post-infection (h)
D
Relative DUSP1 mRNA level
Post-infection (h)
E
siALKBH5 NC si1 si2 si3
DUSP1
1 0.76 0.65 0.55
ALKBH5
1 0.06 0.12 0.19
GAPDH
F
Relative DUSP1 m6A level
siALKBH5 NC si1 si2 si3
G
Relative DUSP1 mRNA level
siALKBH5 NC si1 si2 si3
H
Relative DUSP1 mRNA level
T1/2 siNC = 0.691 h
T1/2 siALKBH5 1# = 0.613 h
T1/2 siALKBH5 2# = 0.576 h
T1/2 siALKBH5 3# = 0.504 h
Post-infection (h)

Figure 2

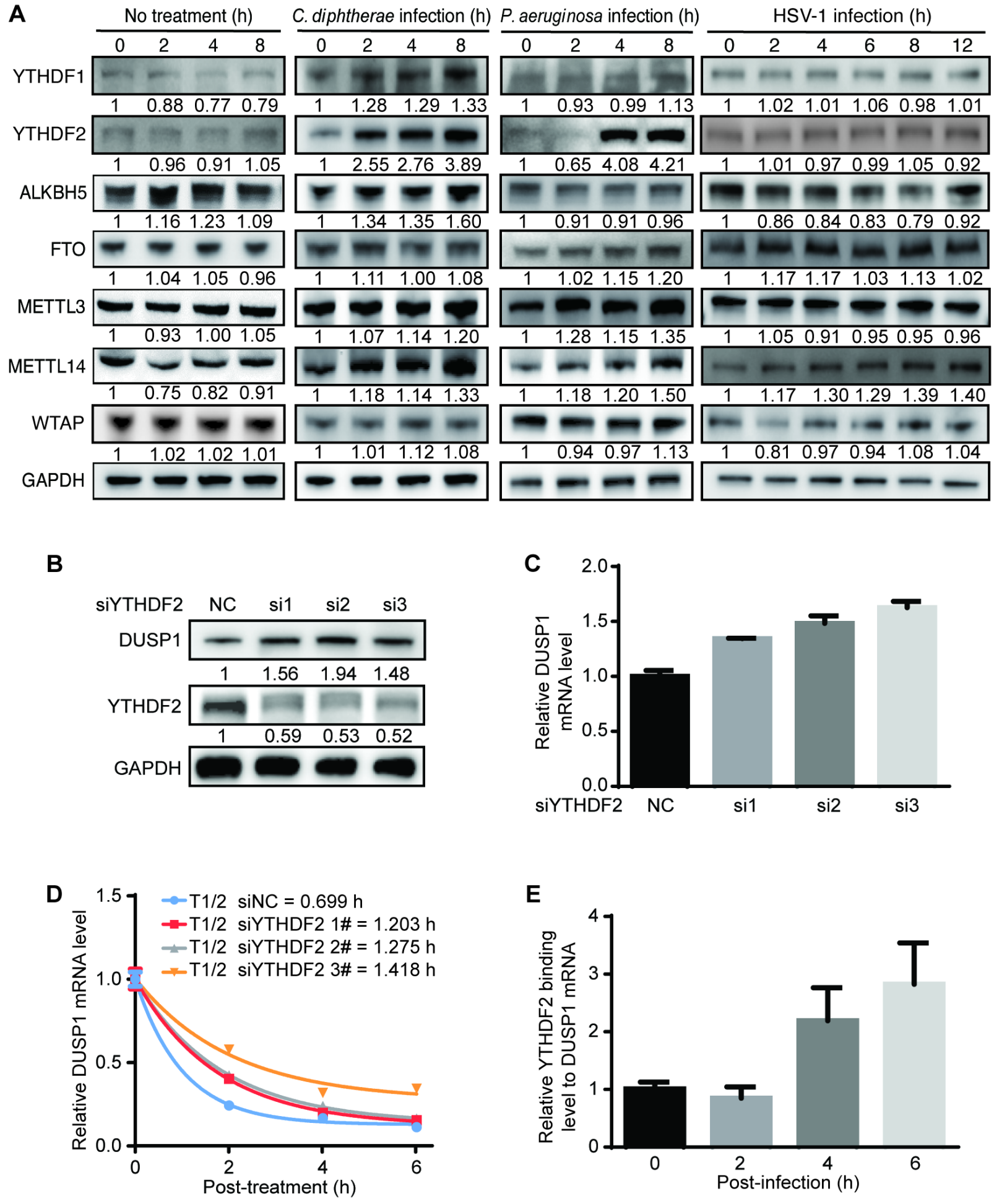

Figure 3

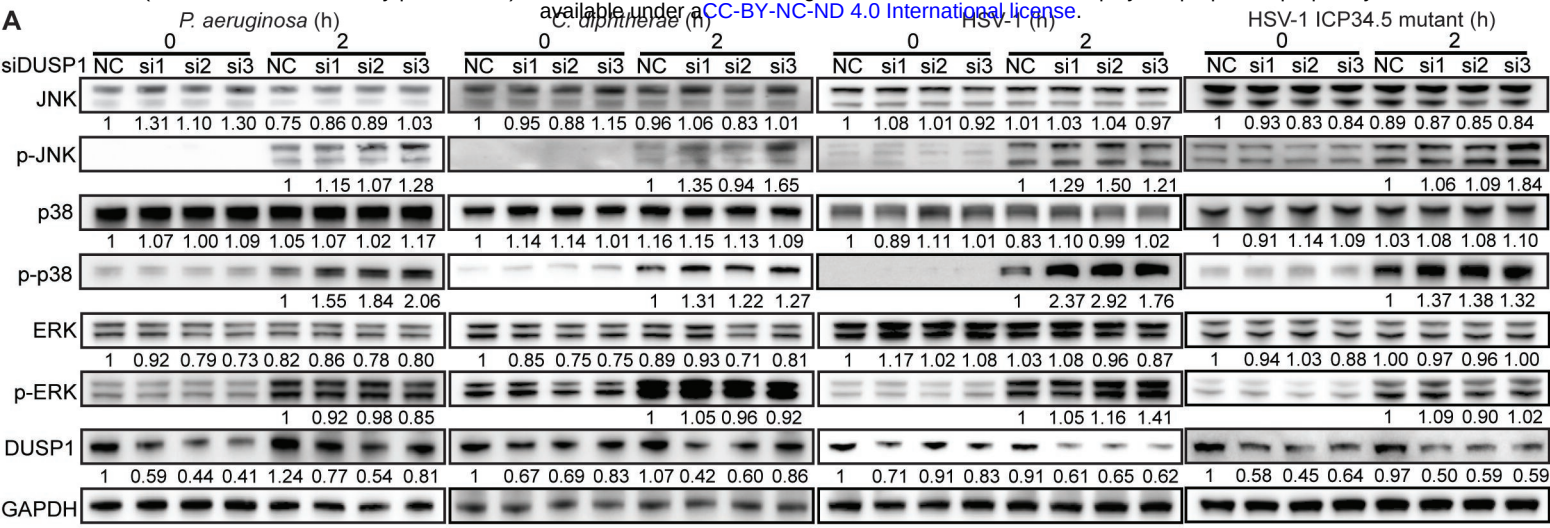

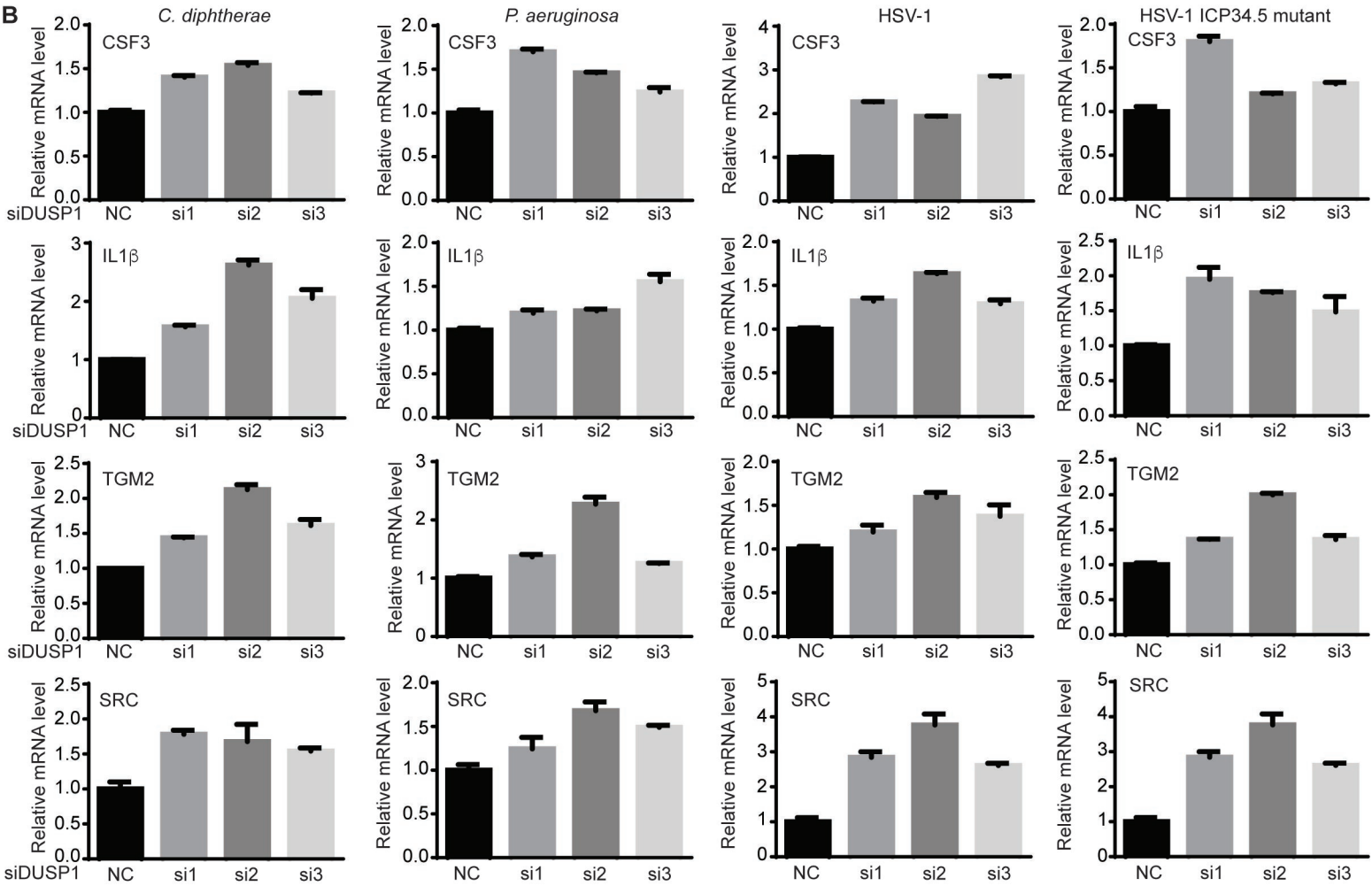

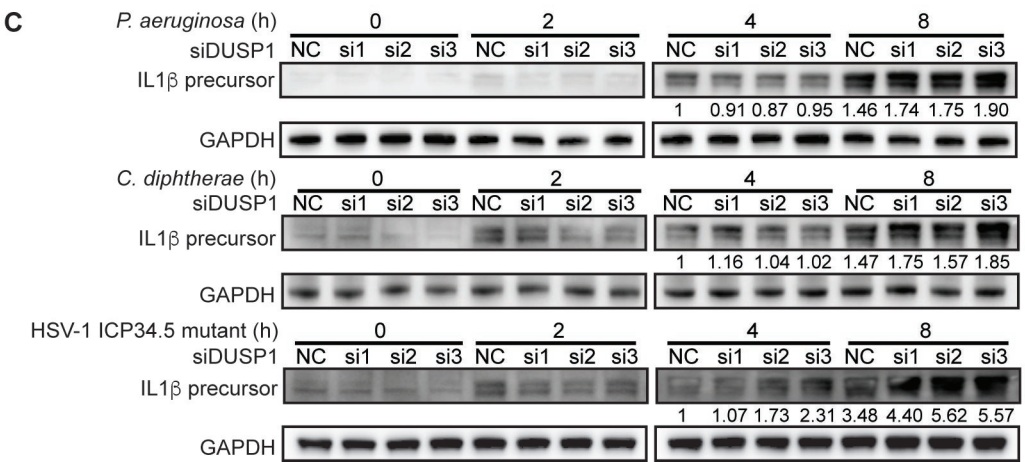

Figure 4

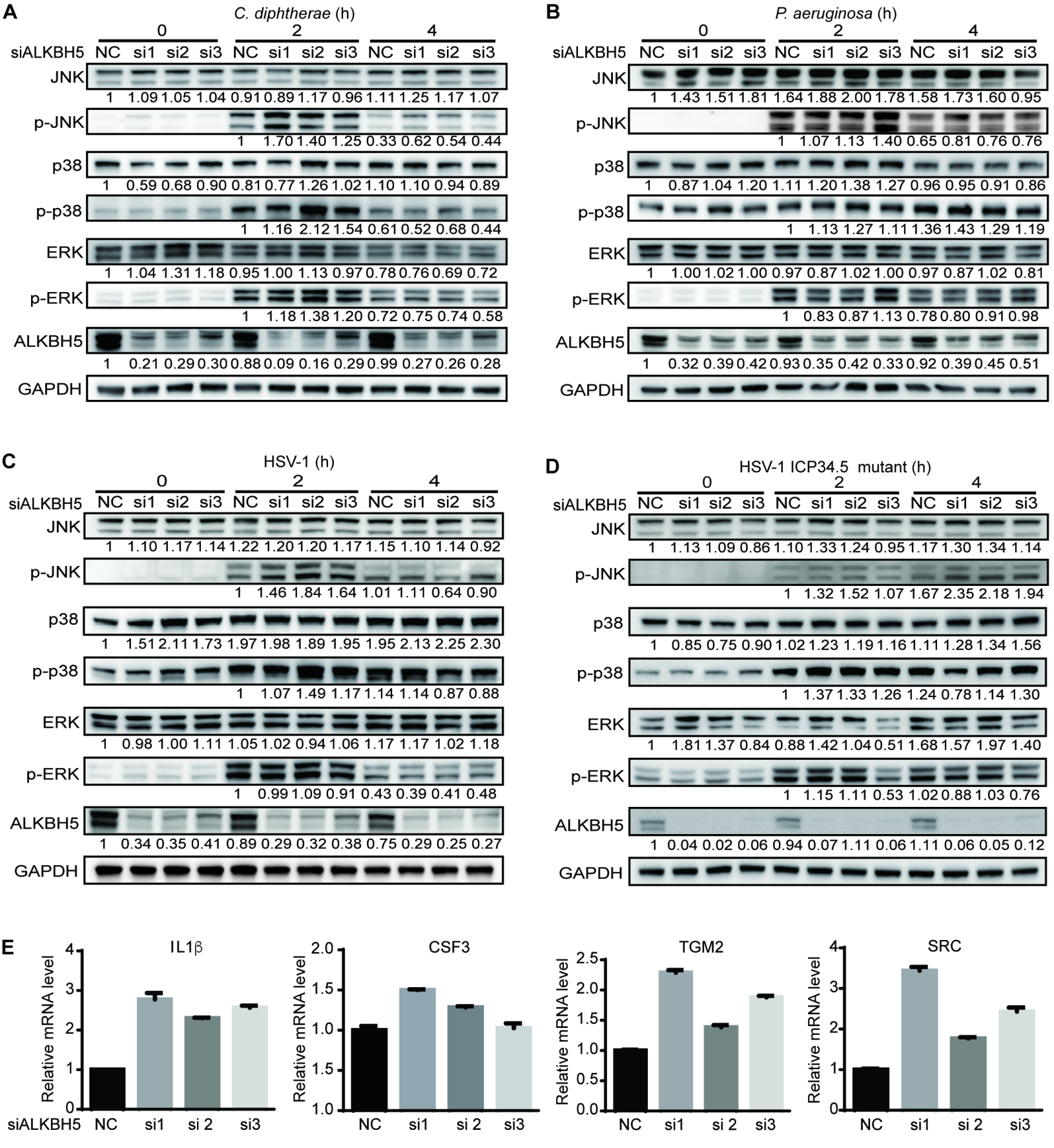

Figure 5

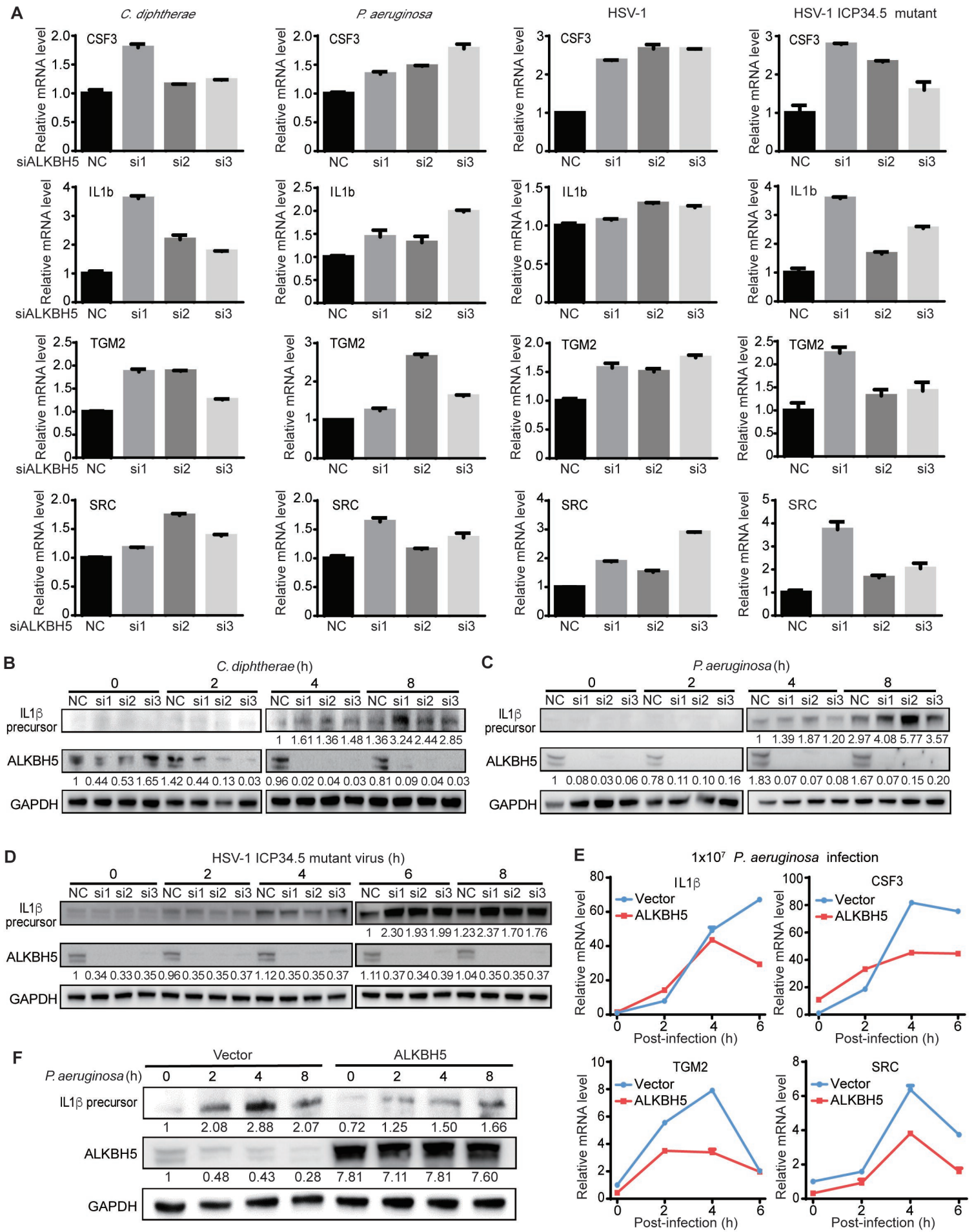
A
C. diphtherae
P. aeruginosa
HSV-1
HSV-1 ICP34.5 mutant
CSF3
IL1b
TGM2
SRC
Relative mRNA level
siALKBH5 NC si1 si2 si3
B
C. diphtherae (h)
0 2 4 8
IL1β precursor
ALKBH5
GAPDH
1 1.61 1.36 1.48 1.36 3.24 2.44 2.85
1 0.44 0.53 1.65 1.42 0.44 0.13 0.03
0.96 0.02 0.04 0.03 0.81 0.09 0.04 0.03
C
P. aeruginosa (h)
1 1.39 1.87 1.20 2.97 4.08 5.77 3.57
1 0.08 0.03 0.06 0.78 0.11 0.10 0.16
1.83 0.07 0.07 0.08 1.67 0.07 0.15 0.20
D
HSV-1 ICP34.5 mutant virus (h)
0 2 4 6 8
1 2.30 1.93 1.99 1.23 2.37 1.70 1.76
1 0.34 0.33 0.35 0.96 0.35 0.35 0.37
1.12 0.35 0.35 0.37 1.11 0.37 0.34 0.39 1.04 0.35 0.35 0.37
E
1x10^7 P. aeruginosa infection
IL1β
CSF3
TGM2
SRC
Vector
ALKBH5
Post-infection (h)
F
Vector
ALKBH5
P. aeruginosa (h)
0 2 4 8 0 2 4 8
IL1β precursor
1 2.08 2.88 2.07 0.72 1.25 1.50 1.66
ALKBH5
1 0.48 0.43 0.28 7.81 7.11 7.81 7.60
GAPDH

Figure 6

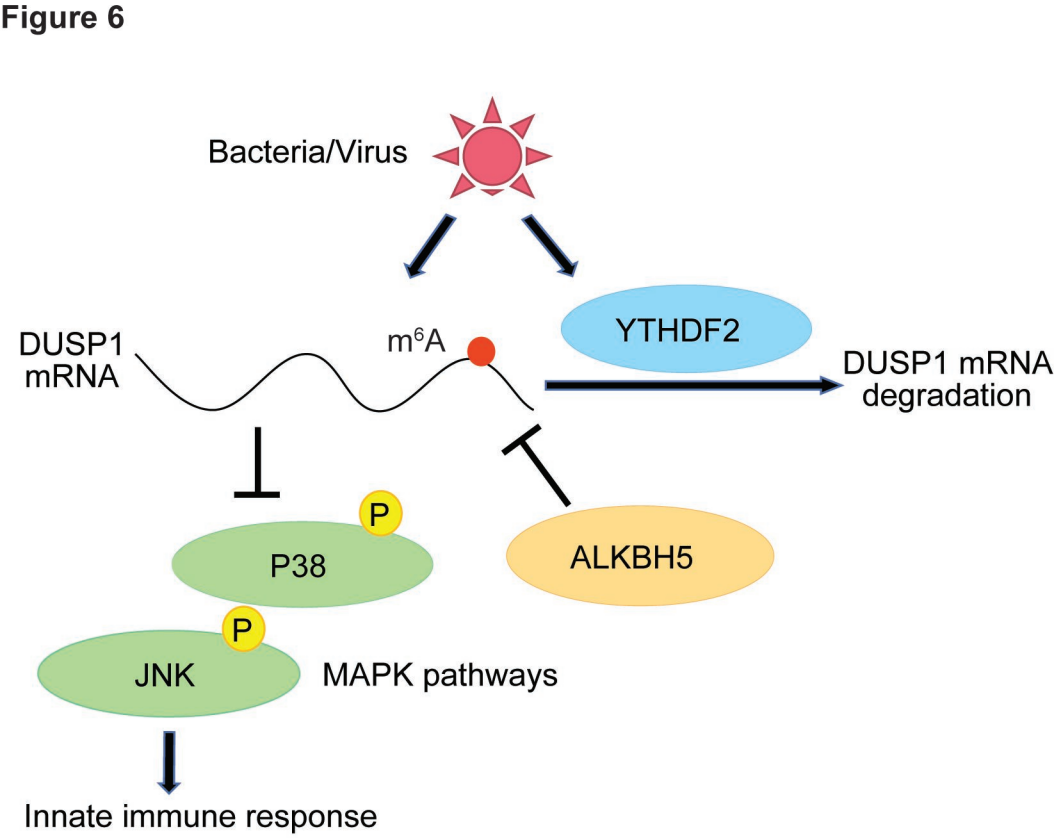
Bacteria/Virus
DUSP1
mRNA
m6A
YTHDF2
DUSP1 mRNA
degradation
P
P38
ALKBH5
P
JNK
MAPK pathways
Innate immune response